

Spin flip probabilities in mesoscopic Ag wires

G. Mihajlović,^{1,*} J. E. Pearson,¹ S. D. Bader,^{1,2} and A. Hoffmann^{1,2}

¹ *Materials Science Division, Argonne National Laboratory, Argonne, IL 60439*

² *Center for Nanoscale Materials, Argonne National Laboratory, Argonne, IL 60439*

(Dated: November 25, 2018)

We have studied spin relaxation in mesoscopic silver wires in the diffusive transport regime via nonlocal spin valve and Hanle effect measurements performed on permalloy/silver lateral spin valves. We find that at low temperatures the ratio between momentum and spin relaxation times is not constant. Nevertheless this observation can be explained with the Elliott-Yafet spin relaxation mechanism by considering the momentum surface relaxation time as temperature dependent. We present a model which allows to determine separately spin flip probabilities for phonon, impurity and surface scattering from the relation between spin and momentum relaxation times or the dependence of the spin diffusion length on the thickness of the wire. Using the first approach we find that the spin flip probability is highest for surface scattering.

PACS numbers: 73.23.-b, 75.40.Gb, 85.75.-d

Understanding how confinement influences physical properties of materials structures is crucial for advancing nanotechnology [1]. Numerous studies have shown that when one or more dimensions of a structure become comparable to a characteristic dimension of the physical process in question (*e.g.*, a mean free path for electron transport) even classical boundary or surface effects can give rise to dramatically different behaviors than those expected for the same bulk material. Examples include magnetoresistance in semiconductor nanostructures (negative *vs.* positive in the bulk) [2] or thermal conductivities in silicon nanowires (orders of magnitude reduction compared to bulk silicon) [3]. In contrast, confinement effects are less evident in metallic transport due to the short mean free path, but manifest themselves often in optical properties [4]. To this end, an important question to be addressed in the emerging area of *spintronics* [5] is how the size of a spin conductor or conditions on its surface affect the transport of spin currents. Due to the relatively long spin diffusion length compared to the mean free path, confinement effects can be more pronounced in spin transport. So far, experiments performed with metallic lateral spin valve (LSV) structures [6, 7], where pure spin currents in a non-magnetic normal metal (N) are generated by diffusion of the non-equilibrium spin accumulation injected from a ferromagnet (F)[8], have focused mostly on determining spin diffusion lengths l_s and spin injection efficiencies P for various combinations of F/N materials, without being able to quantify contributions of different scattering mechanisms to the spin relaxation. In particular, to what extent confinement, which inevitably introduces electron surface scattering, affects the spin relaxation time τ_s is not known [9]. In this Letter we present a model, based on the Elliott-Yafet (EY) mechanism of spin relaxation [10, 11], which allows to separately quantify spin flip probabilities for phonon, impurity and surface scattering in mesoscopic metal wires in the diffusive

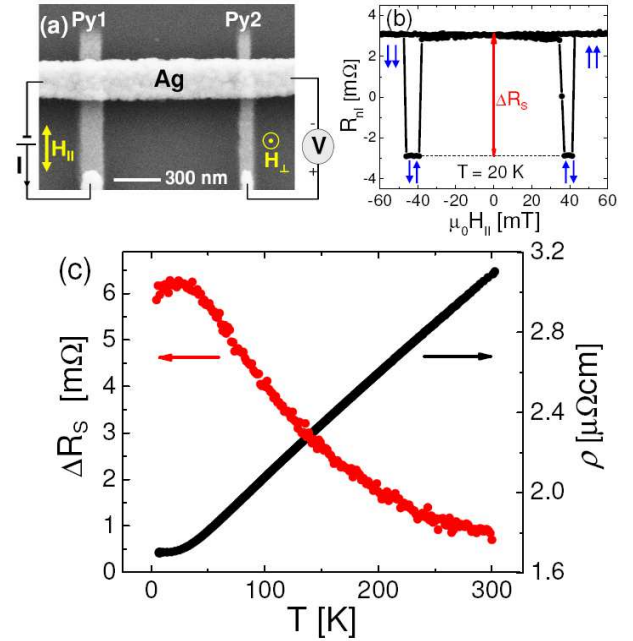


FIG. 1: (Color online) (a) An SEM image of a Py/Ag LSV device adapted to show the nonlocal measurement configuration. Also shown are the directions of H_{\parallel} and H_{\perp} applied in NLSV and Hanle effect measurements, respectively. (b) R_{nl} vs. H_{\perp} at 20 K. Corresponding M orientations of the Py electrodes are shown as blue arrows, while the total ΔR_s signal is highlighted in red. (c) T dependencies of ΔR_s and ρ .

transport regime. By studying spin transport in permalloy (Py)/Ag LSVs we find, using this model, that the spin flip probability is highest for electron scattering off the surface of the Ag wire. Our model may also explain recent experimental results on temperature T [12] as well as thickness dependence of l_s in mesoscopic Cu wires [13].

The Py/Ag LSV devices were fabricated on a SiN (100 nm)/Si substrate by e-beam lithography and shadow mask e-beam evaporation. A scanning electron micro-

scope (SEM) image of a central region of the fabricated device is shown in Fig. 1(a). The two Py electrodes Py1 and Py2 were both 25 nm thick and had different widths of 130 nm and 80 nm respectively, while the bridging Ag wire was 260 nm wide and 80 nm thick. For the results presented in this paper the center to center distance L between Py electrodes was 705 nm. Nonlocal spin valve (NLSV) and Hanle effect measurements were performed by applying an alternating dc current $I = \pm 0.3$ mA from Py1 into the left part of the Ag wire and measuring the voltage V between Py2 and the right end of the Ag wire as a function of parallel H_{\parallel} and perpendicular H_{\perp} magnetic fields, respectively [see Fig. 1(a)].

Figure 1(b) shows the result of the NLSV measurement at $T = 20$ K. The dips in the nonlocal resistance, $R_{nl} = V/I$, due to spin accumulation in Ag, upon switching the magnetization (M) orientation of Py1, are clearly observed. The total magnitude of the difference between the R_{nl} values measured for parallel and antiparallel M orientation of Py electrodes, i.e., ΔR_s is ~ 6.1 m Ω which is a very large signal measured for these LSVs, given the distance $L = 705$ nm between the injector and the detector [14, 15]. Also note that the values of R_{nl} for parallel and antiparallel M orientation of the Py electrodes are almost perfectly symmetric with respect to zero, meaning that they are due to pure spin transport without accompanying R_{nl} signals which may arise from different effects [16, 17].

The large ΔR_s values obtained in these measurements allow to obtain its T dependence by measuring R_{nl} directly as a function of T for parallel and antiparallel remnant M orientations of the Py electrodes, respectively. Fig. 1(c) shows the obtained T dependence of $\Delta R_s = R_{nl}^{\uparrow\uparrow} - R_{nl}^{\downarrow\uparrow}$ and the corresponding conventional electrical resistivity ρ . Clearly, ΔR_s is non-monotonic at low T despite the monotonic decrease of ρ [see Fig. 1(c)]. Similar behavior has been also observed in the case of Py/Cu LSVs [12] and was attributed to the reduction of l_s in Cu due to surface scattering.

In order to determine whether a similar physical mechanism may also cause the behavior observed in our sample, we turned to Hanle effect measurements, since they avoid variabilities between different samples, which are unavoidable in thickness-dependent studies. For Hanle measurements a combined effect of spin precession, relaxation and dephasing leads to characteristic dependence of ΔR_s on H_{\perp} , the so called Hanle resistance R_H , which can be expressed as [18]

$$R_H^{\uparrow\uparrow}(H_{\perp}) = \frac{P^2 \rho D}{A} \int_0^{\infty} \mathcal{P}(t) \cos(\omega_L t) \exp\left(-\frac{t}{\tau_s}\right) dt, \quad (1)$$

for parallel M orientation, and $R_H^{\downarrow\uparrow}(H_{\perp}) = -R_H^{\uparrow\uparrow}(H_{\perp})$ for antiparallel Py electrodes. Here, $\omega_L = g\mu_B\mu_0 H_{\perp}/\hbar$ is the Larmor frequency (g - Lande factor, μ_B - Bohr magneton, μ_0 - magnetic permeability of free space) and

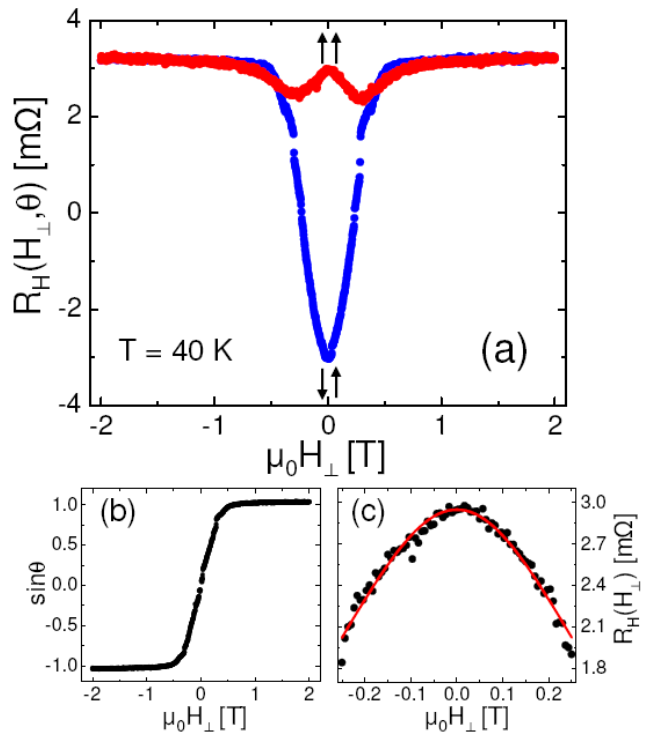


FIG. 2: (Color online) (a) Hanle signals measured at $T = 40$ K for parallel ($\uparrow\uparrow$, red) and antiparallel ($\downarrow\uparrow$, blue) M orientations of Py electrodes. (b) $\sin \theta$ vs. $\mu_0 H_{\perp}$ obtained from data shown in (a) by using Eq. (3). (c) Hanle signal (symbols) at $T = 40$ K obtained from the data shown in (a) by using Eq. (4). The best fit according to Eq. (1) is shown as a red line.

$\mathcal{P}(t) = (1/\sqrt{4\pi Dt}) \exp(-L^2/4Dt)$ is the probability distribution of traveling times t of the injected spins from Py1 to Py2. Thus the Hanle effect measurements allow to determine separately P and τ_s by fitting R_H vs. H_{\perp} data to Eq. (1), if one knows D , ρ , L and A .

Fig. 2(a) shows representative R_H data, obtained at $T = 40$ K for Py electrodes prepared in parallel (red) and antiparallel (blue) M configurations. The difference between the two signals (not shown) exhibits an oscillating sign change as a function of H_{\perp} as expected from the spin precession. However, the behavior in detail is more complicated than expected from Eq. (1). The striking feature of the data in Fig. 2(a) is the strongly asymmetric shape of the two curves with respect to $R_H = 0$, which has not been observed in previously reported Hanle effect measurements in Al [18, 19]. In order to understand this asymmetry, which was observed at all T s, one has to take into account that in addition to precession and dephasing of the spin accumulation, the measured signal also depends on the orientation of the M of Py electrodes with respect to the substrate plane. Namely, M inevitably tilts in the perpendicular direction due to application of H_{\perp} . This decreases the fraction of precessing spin accumulation, and tends to restore the R_H signal to its initial value of $\Delta R_s/2$ for parallel M orientations. When this

effect is taken into account, R_H can be expressed as [18]

$$R_H^{\uparrow(\downarrow)}(H_{\perp}, \theta) = \pm R_H^{\uparrow}(H_{\perp}) \cos^2(\theta) + |R_H(0)| \sin^2(\theta), \quad (2)$$

with "+" and "-" signs corresponding to $\uparrow\uparrow$ and $\downarrow\downarrow$ case respectively. Here θ is the angle between the substrate plane and the direction of the M of Py electrodes, which depends also on H_{\perp} . Based on Eq.(2) one can find

$$\sin^2(\theta) = \frac{R_H^{\uparrow}(H_{\perp}, \theta) + R_H^{\downarrow}(H_{\perp}, \theta)}{2|R_H(0)|}. \quad (3)$$

Fig. 2(b) shows the dependence of $\sin \theta$ on $\mu_0 H_{\perp}$ obtained by using Eq. (3) for the case shown in Fig. 2(a). For sufficiently low $\mu_0 H_{\perp}$ the dependence is linear, but saturates above $\sim \pm 0.5$ T. This dependence is consistent with the Stoner-Wohlfarth model[20] for coherent M rotation with magnetic fields applied along a hard-axis direction. The obtained slope of 2.7 T^{-1} for $\sin \theta$ around zero field corresponds to a demagnetizing factor $N = 0.37$, taking the saturation magnetization for Py $M_s = 1 \text{ T}$. This value agrees reasonably well with the literature one of $N = 0.5$ if one takes into account that the latter is defined for a case of an infinitely long wire. Therefore, we conclude that the asymmetry in the measured R_H curves arises from the tilting of the Py electrode magnetizations out of plane in the direction of H_{\perp} .

From the obtained data, and using Eq. (2), we can thus extract pure Hanle effect signal, i.e. $R_H^{\uparrow}(H_{\perp})$, with

$$R_H^{\uparrow}(H_{\perp}) = |R_H(0)| \frac{R_H^{\uparrow}(H_{\perp}, \theta) - R_H^{\downarrow}(H_{\perp}, \theta)}{2|R_H(0)| - R_H^{\uparrow}(H_{\perp}, \theta) - R_H^{\downarrow}(H_{\perp}, \theta)}, \quad (4)$$

while $R_H^{\downarrow}(H_{\perp})$ is simply $-R_H^{\uparrow}(H_{\perp})$.

Fig. 2(c) shows $R_H^{\uparrow}(H_{\perp})$ obtained by using Eq. (4) for $T = 40 \text{ K}$. The best fit according to Eq. (1) is shown as a red line. Only the region between $\pm 0.25 \text{ T}$ is used for fitting since $R_H^{\uparrow}(H_{\perp})$ obtained this way is not well defined for higher fields due to denominator in Eq.(6) being close to zero. The fit gives $P = 0.207$ and $\tau_s = 14.4 \text{ ps}$, corresponding to $l_s = 564 \text{ nm}$. We repeated this procedure to determine τ_s for several additional T s in the range from 4.5 to 200 K, where the Hanle effect was observed.

Fig. 3 shows the dependence of $1/\tau_s$ on ρ as well as T (see inset). While above $\sim 40 \text{ K}$ $1/\tau_s$ increases linearly with both ρ and T , as expected from the EY mechanism of spin relaxation [10, 11, 21], around $\sim 40 \text{ K}$ it exhibits a minimum, and then slightly increases with decreasing both ρ and T . While similar behavior has recently been observed for Cu wires [12] and qualitatively explained as due to spin flip surface scattering, it is important to emphasize that the conventional approach to surface spin relaxation [22, 23] based on the Fuchs model [24] with a T -independent surface momentum relaxation time τ_e^S , cannot quantitatively explain the nonlinear dependence

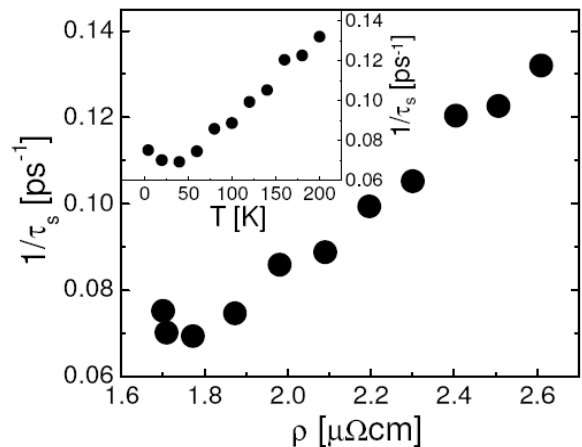


FIG. 3: Dependence of spin relaxation rate on resistivity of the Ag wire. Inset: T dependence of the spin relaxation rate.

of $1/\tau_s$ on ρ , let alone the upturn of $1/\tau_s$ at low T . The discrepancy can be resolved by invoking a concept of T -dependent τ_e^S [25, 26]. Namely, when at least one dimension d of the metallic wire is longer than the bulk electron mean-free path l_e^B (in our case: $34 \text{ nm} < l_e^B < 58 \text{ nm}$ over the whole investigated T range), the τ_e^S , which is the time it takes an electron to diffuse over the distance d is given as $\tau_e^S = d/D_B^2$. Here, $D_B = (1/3)v_F^2\tau_e^B$ is the T -dependent three-dimensional bulk diffusion constant, with v_F and τ_e^B being the electron Fermi velocity and the bulk momentum relaxation time, respectively. The latter is determined by scattering within the bulk of the wire and can be defined as $(\tau_e^B)^{-1} = (\tau_e^{ph})^{-1} + (\tau_e^{imp})^{-1}$, where τ_e^{ph} and τ_e^{imp} are momentum relaxation times for electron scattering off phonons and impurities (including the grain boundaries), respectively. Thus we can write for the total momentum relaxation time τ_e

$$\frac{1}{\tau_e} = \frac{1}{\tau_e^{ph}} + \frac{1}{\tau_e^{imp}} + \frac{1}{3} \left(\frac{v_F}{d} \right)^2 \tau_e^B. \quad (5)$$

Associating to each scattering process its corresponding spin flip probability, i.e., ϵ_{ph} , ϵ_{imp} and ϵ_S , and following the EY proportionality between momentum and spin relaxation times [21], we find

$$\begin{aligned} \frac{1}{\tau_s} &= \frac{\epsilon_{ph}}{\tau_e^{ph}} + \frac{\epsilon_{imp}}{\tau_e^{imp}} + \frac{1}{3} \left(\frac{v_F}{d} \right)^2 \epsilon_S \tau_e^B \\ &= \frac{\epsilon_{ph}}{\tau_e^B} + \frac{1}{3} \left(\frac{v_F}{d} \right)^2 \epsilon_S \tau_e^B + \frac{\epsilon_{imp} - \epsilon_{ph}}{\tau_e^{imp}}. \end{aligned} \quad (6)$$

Eq. (6) explains naturally the nonlinearity in $1/\tau_s$ vs. ρ (since τ_e^B within this model depends nonlinearly on ρ) and, even more significantly, it allows for the upturn in $1/\tau_s$ at low T , since the first and second term in the Eq. (6) have different dependence on ρ . Also, based on Eq. (6), one can determine ϵ_{ph} , ϵ_{imp} and ϵ_S by fitting the $1/\tau_s$ vs. $1/\tau_e^B$ dependence, which can be obtained by

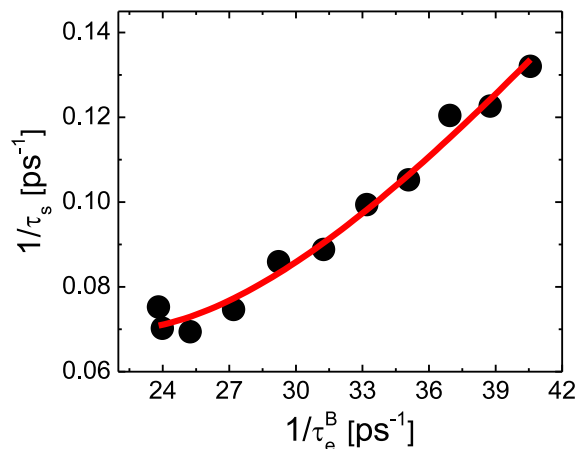


FIG. 4: (Color online) Dependence of spin relaxation rate in the Ag wire on the bulk momentum relaxation rate (symbols). The fit to the data according to Eq. (6) is shown as a red line.

performing T -dependent spin transport measurements as the ones shown in Fig. 3.

Fig. 4 shows the plot of $1/\tau_s$ vs. $1/\tau_e^B$ (black circles), where τ_e^B is obtained as $\tau_e^B = (1 - \sqrt{1 - 4a\tau_e^2})/(2a\tau_e)$ with $a = (v_F/d)^2/3$, and $\tau_e = m/(ne^2\rho)$ determined from the measured ρ . The best fit according to Eq. (6) is shown as a red line. We find $\epsilon_{ph} = (7.5 \pm 1.3) \times 10^{-3}$, $\epsilon_S = (3.6 \pm 1.2) \times 10^{-2}$ and $\epsilon_{imp} = (-3.4 \pm 4.4) \times 10^{-3}$. These values show that the spin flip probability is highest for surface scattering and weakest for scattering on impurities ($< 1 \times 10^{-3}$)[28]. Also note that the value for ϵ_{ph} agrees well with a previously reported value of $\epsilon_{ph} = 2 \times 10^{-3}$ for Cu wires (about 4 times smaller value consistent with Cu being a lighter element) [9] as well as the value of $\epsilon_{ph} = 2.9 \times 10^{-3}$ obtained from electron spin resonance measurements on bulk Ag [27].

Based on this model, we can also predict the thickness dependence of l_s . Multiplying Eq. (6) by $1/D$, where D is the total diffusion constant, one finds

$$l_s = \frac{d}{\sqrt{\alpha d^2 + \beta}}, \quad (7)$$

where in the low T limit, when $\tau_e^B \simeq \tau_e^{imp}$, $\alpha = \epsilon_{imp}/(D\tau_e^{imp})$ and $\beta = (v_F^2\epsilon_S\tau_e^{imp})/(3D)$. In the high T limit, when phonon scattering is non-negligible, $\alpha = \epsilon_{imp}/(D\tau_e^{imp}) + \epsilon_{ph}/(D\tau_e^{ph})$ and $\beta = (v_F^2\epsilon_S\tau_e^B)/(3D)$. These relations also allow to determine ϵ_{ph} , ϵ_{imp} and ϵ_S by fitting the thickness dependence of the spin diffusion length obtained for low and high T . However, such measurements always require the use of several samples, which introduces additional experimental uncertainties.

In conclusion, we have studied the spin relaxation in a mesoscopic Ag wire in the diffusive transport regime, and observed a nonlinear dependence of the spin relaxation rate on resistivity. This observation cannot be explained quantitatively with the Elliott-Yafet mechanism

of spin relaxation by a conventional approach, which considers momentum relaxation time for surface scattering as temperature independent. We present a simple model which explains these observations with the Elliott-Yafet mechanism by adding a temperature dependence to the surface relaxation. This enables us to quantify spin flip probabilities for phonon, impurity and surface scattering respectively. We find that the spin flip probability in the case of the Ag wire is strongest for electron scattering off surfaces.

We thank Roland Winkler, Karel Vyborny, and Oleksandr Mosendz for many stimulating discussions and Leo Ocola and Ralu Divan for assistance with nanofabrication. This work was supported by the U.S. Department of Energy, Office of Science, Office of Basic Energy Sciences, under contract No. DE-AC02-06CH11357.

* Electronic address: mihajlovic@anl.gov

- [1] S. D. Bader, Rev. Mod. Phys. **78**, 1 (2006).
- [2] T. J. Thornton, M. L. Roukes, A. Scherer, and B. P. Van de Gaag, Phys. Rev. Lett. **63**, 2128 (1987).
- [3] A. I. Boukai, Y. Bunimovich, J. Tahir-Kheli, J. -K. Yu, W. A. Goddard III, and J. R. Heath, Nature (London) **451**, 168 (2008).
- [4] W. L. Barnes, A. Dereux, and T. W. Ebbesen, Nature (London) **424**, 824 (2003).
- [5] I. Žutić, J. Hoffmann, and S. Das Sarma, Rev. Mod. Phys. **76**, 323 (2004).
- [6] F. J. Jedema, A. T. Filip, and B. J. van Wees, Nature (London) **410**, 345 (2001).
- [7] Y. Ji, A. Hoffmann, J. S. Jiang, and S. D. Bader, Appl. Phys. Lett. **85**, 6218 (2004).
- [8] M. Johnson and R. H. Silsbee, Phys. Rev. Lett. **55**, 1790 (1985).
- [9] F. J. Jedema, M. S. Nijboer, A. T. Filip, and B. J. van Wees, Phys. Rev. B **67**, 085319 (2003).
- [10] R. J. Elliott, Phys. Rev. **96**, 266 (1954).
- [11] Y. Yafet, in *Solid State Physics*, edited by F. Seitz and D. Turnbull (Academic, New York, 1963), Vol. 14.
- [12] T. Kimura, T. Sato, and Y. Otani, Phys. Rev. Lett. **100**, 066602 (2008).
- [13] M. Erekhinsky, A. Sharoni, F. Casanova, and I. K. Schuller, arXiv:0908.3508v2.
- [14] R. Godfrey and M. Johnson, Phys. Rev. Lett. **96**, 136601 (2006).
- [15] T. Kimura and Y. Otani, Phys. Rev. Lett. **99**, 196604 (2007).
- [16] F. Casanova, A. Sharoni, M. Erekhinsky, and I. K. Schuller, Phys. Rev. B **79**, 184415 (2009).
- [17] G. Mihajlović, J. E. Pearson, M. A. Garcia, S. D. Bader, and A. Hoffmann, Phys. Rev. Lett. **103**, 166601 (2009).
- [18] F. J. Jedema, H. B. Heersche, A. T. Filip, J. J. A. Baselmans, and B. J. van Wees, Nature (London) **416**, 713 (2002).
- [19] S. O. Valenzuela and M. Tinkham, Nature (London) **442**, 176 (2006).
- [20] E. C. Stoner and E. P. Wohlfarth, Philos. Trans. R. Soc. London, Ser. A **240**, 599 (1948).

- [21] J. Fabian and S. Das Sarma, *J. Vac. Sci. Technol. B* **17**, 1708 (1999).
- [22] P. E. Lindelof and S. Wang, *Phys. Rev. B* **33**, 1478 (1986).
- [23] J. -Q. Wang and G. Xiao, *Phys. Rev. B* **51**, 5863 (1995).
- [24] E. H. Sondheimer, *Adv. Phys.* **1**, 1 (1952).
- [25] A. J. Watts and J. E. Cousins, *Phys. Stat. Sol.* **30**, 105 (1968).
- [26] I. G. Zamaleev and E. G. Kharakhashyan, *JETP Lett.* **27**, 641 (1978).
- [27] F. Beuneu and P. Monod, *Phys. Rev. B* **13**, 3424 (1976).
- [28] Note that the negative sign of the fitted ϵ_{imp} is meaningless and within the errorbar. Thus we do not have sufficient sensitivity to determine ϵ_{imp} .